

# Design of a Solar Sand Printer

---

*Internship at the Working Group on Development Techniques*

Author: Menno-Jan Rietema

Supervisors:

ing. C.Vos of Engineering Consultancy *Vos Solutions*

Ir. E. de Jong

External supervisor:

dr.ir. W.W.Wits of the *University of Twente*

Period: 17-10-2012 to 30-12-2012

## Table of Contents

Preface.....	4
1 Introduction.....	5
1.1 Requirements of internship.....	5
1.2 Current state of art.....	6
1.3 Planning internship/ordering materials .....	7
2 Basic calculations.....	9
2.1 Silicon melting behaviour .....	9
2.2 Required energy to melt sand .....	11
2.3 Energy losses during operation .....	12
2.3.1 Radiation.....	12
2.3.2 Reflection.....	13
2.3.3 Melting the previous layer .....	13
2.3.4 Conduction .....	13
2.3.5 Convection.....	13
2.4 Incoming solar energy .....	14
2.4.1 Solar irradiation .....	14
2.4.2 Lens efficiency .....	15
2.5 Energy balance and production rate .....	15
2.6 Optimisation and lens choice .....	15
2.6.1 Lens choice .....	15
2.6.2 Optimisation .....	15
3 Designing .....	17
3.1 Goal of design.....	17
3.2 Choice of mechanical designs.....	17
3.2.1 Concentrating sun light .....	17
3.2.2 Moving hot spot versus product .....	18
3.2.3 Tracking of the sun .....	18
3.3 Conceptual design .....	19
3.4 Conceptual electrical drive system.....	20
4 Construction of design .....	22
4.1 Refining concept.....	22
4.2 Calculating bearing loads and rail thickness.....	28
4.3 Calculating required motor force/choosing motors .....	29

4.3.1	Sun tracking (rotation of table) .....	29
4.3.2	Z-movement .....	29
4.3.3	XY- movement .....	33
4.4	Installation of electronics board.....	34
4.4.1	Sun tracking.....	35
4.5	Building of concept.....	36
5	Conclusion and recommendations.....	39
5.1	Recommendations.....	39
6	Sources .....	41
7	Appendix.....	43

## Preface

### SIMPLE IS NOT EASY

The art of making things has always inspired me. This was the main reason why I chose to follow the study Mechanical Engineering. In my opinion this was the best study that could teach its students this art including the mechanical, mathematical and process related backgrounds. This was also the reason why I joined the student association 'the Working Group on Development Techniques' (WOT) not long thereafter. Its members are driven by the art of making things. The target group for all the designs made by the WOT are the developing countries. As is usually suspected after reading the name, the work of the WOT includes 'the standard' set of development techniques such as hand pumps, wind mills for electricity and water, and solar water heaters. But to the surprise of the most, the designs of the WOT do not limit themselves to those things. The designs are influenced by time, new technologies and changing demands of people all around the world. Technologies that were only futile dreams in the past are now being realised at the WOT. For example, a small box with electronics, that can send wireless information about pump usage, performance and ground water levels. As soon as it detects that the pump is broken, it sends a message to the service centre asking for reparation. Or another example: of a smart water tap. People can use their cell phone to open the tap, and payment for each Litre is deducted from their mobile account. In all of these fantastic old and new ideas, a key element is the straightforwardness of the eventual product. They should be as simple as possible in fulfilling their goal, without being too simple.

An amazing idea was the work of Markus Kayser. He managed to build a 3d printer to sinter sand into 3d sculptures. Since there was only a very limited amount of information on his design available, the idea rose to build a similar printer at the WOT, and investigate if such a printer could be used in developing countries for prototyping or production. This would remove the 'art status' of the project, and add a sense of purpose.

In the last few months, a new machine has developed in the working place of the WOT. Currently not yet finished, but for sure it will be able to print figures of sand coming summer. It has been a real challenge to design the machine, and I experienced in real live that designing things simple is not always easy.

Many volunteers at the WOT helped me with thinking, designing and constructing, for which many thanks. My special thanks go to both of my supervisors at the WOT. Chris helped me a lot with his insights in designing, and spent many days working with me in the workshop. Only a few of these days did not end with conversations about life under the joy of a Grolsch beer. Bertus helped me a lot with selecting the right electronics, motors and gearboxes and checking the calculations that I made.

My thanks also go to Thom, who helped me by programming the sun tracking system. To Freddy, who was most of the time during my internship present at the WOT and always available for questions. And at last to Mario, who helped me many days in the workshop, always with a positive mood and ready to help when things went different than planned.

# 1 Introduction

The construction of buildings has a high demand on assets as energy, materials, labour and costs. A reduction in any of these assets would be welcomed by many people, especially at the bottom of the pyramid. A promising technology in this field is 3D printing. However this production technology is especially useful for rapid prototyping and not for mass production, it might replace labour intensive building processes like masonry. 3D printing can enable companies to directly create designs from their CAD drawings, without requirements of additional labourers.

If this high end production technology can be operated with solar (thermal) energy, and uses low cost and widely available materials as sand, it is a very promising building technique for many people in many places around the world. Already there are interesting examples of creative people that are sintering sand with focussed solar thermal energy to form artworks [1]. The time is here to take this creativity to the next level, and investigate the possibility to use it for serious construction.

For this reason the Working Group on Development Techniques (in Dutch: Werkgroep OntwikkelingsTechnieken; WOT) designed this fulltime project proposal for a student who wants to investigate the possibilities of solar sand printing for production of housing in developing countries. This project combines knowledge of a mechanical engineering student of the University (material knowledge, design skills) with knowledge and experience of the WOT (smart creation, design for the poor, development technology).

## 1.1 Requirements of internship

This project is a feasibility study on the use of the sun and sand to produce houses. To achieve a useful output for the WOT, the project has two sets of requirements. The first set is about the topic and the design. The second set is on the expected output from the project.

### 1.1.1.1 Requirements on design

These can be adapted and refined in conversation with the WOT and are meant to make this technology user friendly and accessible for people at the bottom of the pyramid. The demands for the design are:

- Use of solar energy
- Use of low cost materials as input, such as sand
- Printing speed is synchronised with solar intensity
- Track solar position automatically
- Scalable/adaptable to print houses or main parts of it

The following guidelines can be kept in mind to make this production technique suitable for people in developing countries.

- Design is transportable, so that transportation of produced parts is avoided
- Design is robust; no extreme wear or clogging due to sand or sun

### 1.1.1.2 Requirements on outcome

This set of requirements is about the products/work that the student has to deliver. If the outcome of the research is positive, this can be the basis of further investigation.

- Feasibility study on Solar Sand Sintering for creating structures
  - o Literature study on strength of formed material
  - o Calculations on required time, energy and costs per structure
  - o Design of printing concepts
- Build proof of concept<sup>1</sup>
- Test concept and strength of formed artefact<sup>1</sup>

## 1.2 Current state of art

Below some examples are given of inspiring initiatives on the interface of printing and house manufacturing.

### Markus Kayser [1]

This designer created a machine that is capable of sintering sand into a 3D sculpture using solar energy. His design is promising and inspiring for larger artefacts.



Figure 1: Markus Kayser's SolarSinter , the sintering and a finished product [1]

<sup>1</sup> Given the time span of only 3 months, the concept cannot be manufactured with great detail. Designing and manufacturing a part of the total concept is probably the most realistic option. Printing a simple artefact (a beam or cylinder for example) is already a useful achievement for further study. This can be arranged in consultation with the coordinator at the WOT.

### D-Shape [2]

The company D-Shape developed a huge free form printer for buildings. They use sand and inorganic binder to create sandstone like buildings.

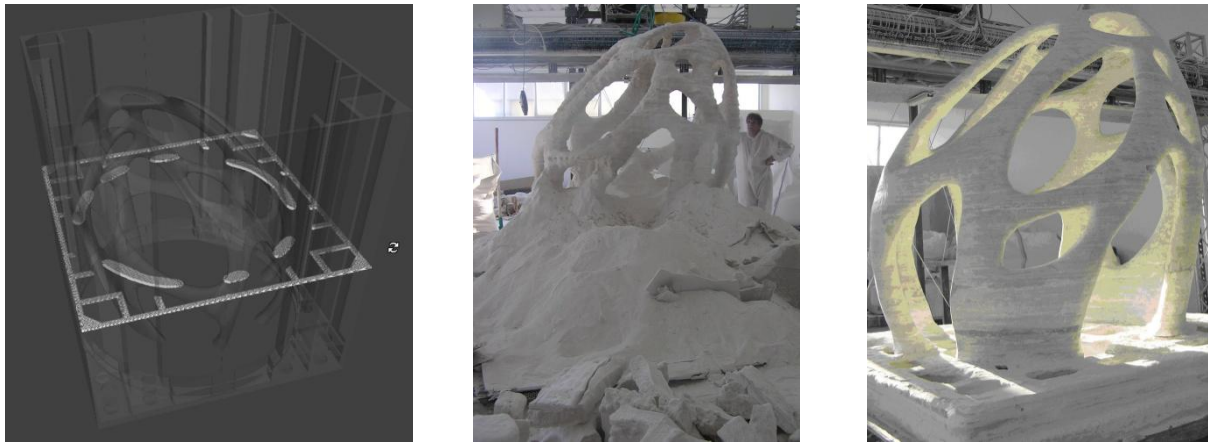


Figure 2: The Radiolaria, from CAD drawing to physical product by “simply pressing the enter-key on the keypad” [2]

### Contour Crafting [3]

The overarching vision for the Center for Rapid Automated Fabrication Technologies (CRAFT) is to develop the science and engineering needed for rapid automated fabrication of objects of various size up to mega-scale structures such as, boats, industrial objects, public art and whole building structures. The aim is to build structures using Contour Crafting, a fabrication technology developed by Dr. Behrokh Khoshnevis of the University of Southern California.

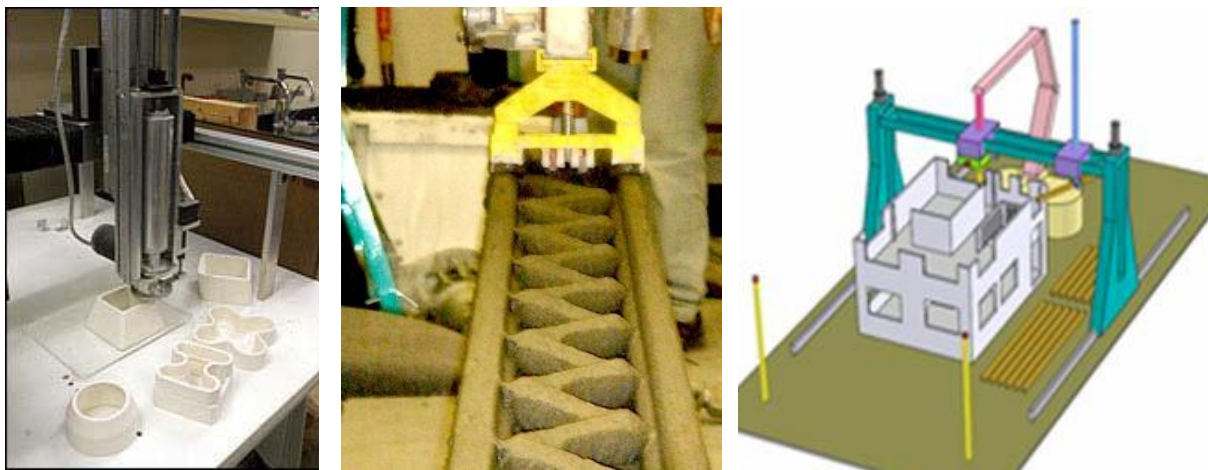


Figure 3: Contour Crafting of small artefacts, a wall and visualisation of Contour Crafting a whole building [3]

## 1.3 Planning internship/ordering materials

The duration of the internship will only take 10 weeks. For this reason a strict planning is necessary.

Week/ day	1	2	3	4	5	6	7	8	9	10
Monday	Finish Chapter 2	Design concepts	Choose concept Prepare construction	Building concept			Testing concept and materials Refine concept			Finish
Tuesday	Order									
Wednesday	long term									
Thursday										

Friday	materials		Order short term materials			
--------	-----------	--	----------------------------	--	--	--

Task \ Week	1	2	3	4	5	6	7	8	9	10
Calculations	■									
Order lenses		■								
Desing mechanic concepts		■	■	■						
Design electrical driver			■	■						
Design CAD conversion			■	■	■					
Choice of mech. concept			■							
Construction of mech. design				■	■	■	■	■		
Construction el. design						■	■	■	■	
Testing of design								■	■	
Finishing report									■	■

## 2 Basic calculations

The main goal of the 3D printer is to construct artefacts with sand that is freely available in a lot of countries. This chapter describes the process of sintering sand, and the required energy for this process.

The source of energy for printing is the sun. A lens will be used to concentrate this energy, so that one layer of sand sticks to a previous layer.

The main amount of the printed mass is molten into a fluid bed. This is necessary because the concentrated sunlight cannot pass its energy to loose sand just below the printing surface, except by conduction. A sintered layer that is only connected on the edges of the sand grains cannot conduct so much energy that the sand below will be sintered as well. For this reason most of the mass that needs to be printed, needs to be melted as well.

### 2.1 Silicon melting behaviour

In order to know the required energy for the process of melting sand, first the chemical properties of sand must be known. Also some knowledge about glass making is preferred, since this well known process is very similar to 3D glass printing.



Figure 4: Dutch sand, mainly consisting of quartz grains with small impurities of iron[4]

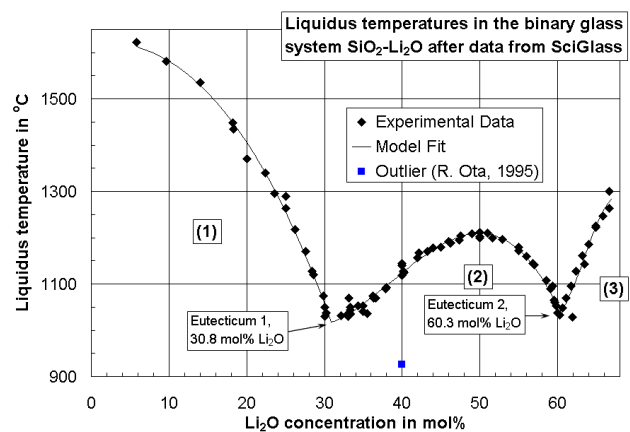


Figure 5: Liquidus temperatures in binary glass system  $\text{SiO}_2\text{-Li}_2\text{O}$  [5]

When a silicon dioxide mixture (such as sand) is heated, it passes a glass transition temperature. This is a viscous state between solid and fluid. When the temperature raises more, the liquidus temperature is reached. Above this temperature all the material is homogenous and liquid at equilibrium.

The liquidus temperature of glass as a function of the  $\text{Li}_2\text{O}$  concentration is given in Figure 5 [5]. As can be seen, the liquidus temperature of the mixture changes highly with the amount of additives to silicon dioxide. The additives can make a eutectic mixture, where the combined melting point is lower than both of the separate melting points.

So, to know the exact melting point, the exact quantity of the components in the sand must be known. Otherwise the only valid statement can be that the temperature on which sand will fluidize is somewhere below  $1700^\circ\text{C}$ , depending on the additives.

### Silver sand

From high grade silver sand is known that it exists for more than 99.6% out of silicon dioxide. It is used for glass manufacturing, and does not contain iron, aluminium or organic contamination [6]. In the Netherlands this sand is found on some places in Limburg as eolic sand, what means that it is transported by wind. 23 to 2.6 million years ago this sand was found as impure river sand, but humus acids eroded all elements except silicon dioxide. Since this process started after sedimentation of the sand, this sand is called post sedimentary silver sand. As can be seen in Figure 5, and found in other literature [7], sand with this composition has a melting point of 1670°C or 1717°C, depending on the crystalline structure of SiO<sub>2</sub>. Since it is almost a pure mixture, it has no real glass transition.

### Soda lime silica mixture

During the Roman Empire glass was made from sand that was found on a few specific beaches, mixed with soda and lime. In the glass furnaces of that time, a temperature of 1000°C to 1200°C at maximum could be reached [8]. Current soda lime glass that is found in bottles and windows is a mixture of approximately 74% SiO<sub>2</sub>, 13% Na<sub>2</sub>O, 10.5% CaO, and minor fractions of metal oxides. The glass transition temperature is around 560 °C and the liquidus temperature around 1040°C. This is a relatively low temperature. Commonly the furnace is heated up to 1575°C.

### Sahara sand

Since the project is especially valuable for countries with a lot of sun and sand, Sahara sand properties are regarded as well. Sand sample analyses from a study in 2006 are given in Figure 6 [9].

Elements as oxides	Cairo 2		Cairo 3		Agadez		Morocco	
	wt-%	sd	wt-%	sd	wt-%	sd	wt-%	sd
SiO <sub>2</sub>	55.2	0.08	62.0	0.06	79.4	0.31	70.22	0.17
Al <sub>2</sub> O <sub>3</sub>	7.7	0.01	9.4	0.01	11.5	0.06	8.37	0.01
CaO	24.3	0.05	13.9	0.01	0.7	0.01	11.47	0.02
MgO	2.9	0.03	4.7	0.04	0.4	0.00	2.26	0.01
Fe <sub>2</sub> O <sub>3</sub>	4.5	0.02	5.0	0.02	2.0	0.01	3.63	0.03
K <sub>2</sub> O	1.18	0.003	1.7	0.00	3.6	0.01	2.04	0.01
Na <sub>2</sub> O	1.1	0.18	1.1	0.01	2.2	0.13	0.52	0.02
P <sub>2</sub> O <sub>5</sub>	0.2	0.01	0.2	0.00	0.0	0.01	<0.1	
TiO <sub>2</sub>	1.4	0.07	1.2	0.02	0.3	0.01	0.81	0.05
Loss of ignition	19.1		16.8		2.7		12.1	

Figure 6: Element analysis of desert sand samples by X-ray fluorescence analysis calculated as oxides (sd = standard deviation) [9].

To get estimate the right properties, programs can be downloaded to analyse properties of glass mixtures. According to the program of EcoGlass [10], the sample mixtures have the properties listed in Figure 7.

Sample	T <sub>g</sub> [°C]	T <sub>l</sub> [°C]
Cairo 2	742	893
Cairo 3	679	877
100% SiO <sub>2</sub>	605	852

Figure 7: Properties of Saharan sand according to EcoGlass software

These results however seem to be far too low. To check this, a mixture of 100% SiO<sub>2</sub> is analysed. The result for the liquidus temperature is almost 1000 degrees off from the expected 1700 degrees Celsius.

After this, a check is done with the program of Pirika [11]. This yields approximately the same results. This program uses the same database [12] as the Excel program GlasstLCalc [13]. This last program reveals the deviation of the expected values. The validity of the data (that is probably the same for all mentioned programs) is outside the amounts of the composition of Sahara sand. If more chemicals are added to the sand to get a transparent glass, these programs might be very interesting to predict the melting points, required energy and the mechanical properties of the printed glass.

## 2.2 Required energy to melt sand

Because there is not a clear melting point of sand, and latent energies cannot be found in literature, two estimates are made to predict the required energy. One is a lower bound, which is given by the energy to melt regular glass. The higher bound is the estimation to melt pure silica.

### Energy to form glass

For regular soda-lime glass produced in a conventional furnace, the rate of energy into the glass batch is 8.16 MW for a continuous production rate of 2.9 kg/s [14]. The energy to melt glass is then calculated to be:

$$8160/2.9=2814 \text{ KJ/kg}$$

### Energy to melt pure silica

The melting point of pure silica is around 1700 degrees C. Because most of ingredients in sand will lower the melting point, up to 1000 degrees C, this is regarded a high estimate for the required energy to melt sand. The specific energy is assumed to be constant during the trajectory and the same as that of sand: 0.80 KJ/kg K. The latent heat of fusion for pure silica is found to be 1926 KJ/kg [15]. Assuming an ambient temperature of 20 degrees C, the energy to melt silica is calculated to be:

$$0.80 \cdot 1 \cdot 1680 + 1926 = 3270 \text{ KJ/kg}$$

*Note: with average sand this amount of energy will be slightly higher, because of chemical reactions of some components in the sand.*

## 2.3 Energy losses during operation

The losses that occur when melting sand are given in Figure 8. This figure represents a cross-sectional view of the sand layer that is printed. In the next subchapters the heat flows are described and calculated or estimated.

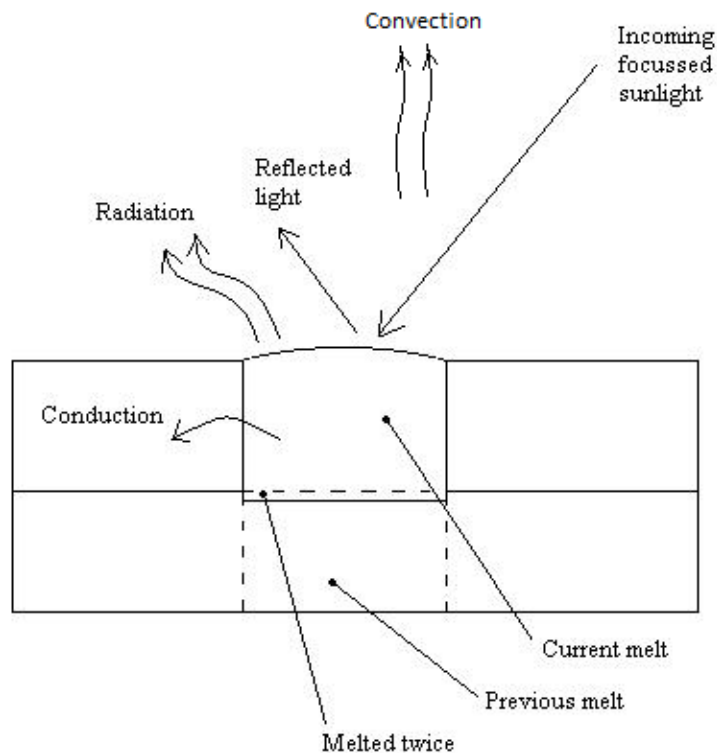


Figure 8: Cross-section of the printed layer with energy flows.

### 2.3.1 Radiation

Because of the relatively high temperature of melted glass, it is assumed that the main energy loss is caused by radiation. The law of Stefan-Boltzmann describes the energy loss due to radiation:

$$q_{\text{rad}} = \varepsilon \cdot \sigma \cdot (T_h^4 - T_c^4) \cdot A$$

where:

$\varepsilon$  = emissivity of the object = 0.76 for sand [16]

$\sigma$  = Stefan-Boltzmann Constant =  $5.6703 \cdot 10^{-8} \text{ W/m}^2 \cdot \text{K}^4$

$T_h$  = hot body absolute temperature = 1973.15 K

$T_c$  = cold surroundings absolute temperature = 300 K

$A$  = area of the object

With an assumed hot focal point with a radius of 1 cm, the radiating surface equals  $\pi \cdot r^2 = \pi \cdot 10^{-4} \text{ m}^2$ , the continuous rate of energy loss by radiation is then calculated to be  $q_{\text{rad}} = 205 \text{ W}$ .

*Note: The result of the loss through radiation is linear dependant of the area of the focus point. If the focal spot has a radius of 2 cm, the energy loss by radiation equals 820W. This shows that the energy loss is highly dependent on the accuracy of the machine assembly and the precision of the lens.*

### 2.3.2 Reflection

The reflectivity coefficient  $\alpha_{\text{sand}}$  of typical Sahara sand is around 0.40 [17]. This means that 40 percent of the incident sunlight is reflected. Thus,  $\eta_{\text{reflection}} = 0.60$ .

### 2.3.3 Melting the previous layer

Because each layer needs to be melted onto the previous layer, a fraction of the previous layer has to be melted as well. It is assumed that 5% of the material is melted twice because of this phenomenon. Thus,  $\eta_{\text{melt}} = 0.95$ .

### 2.3.4 Conduction

The conduction coefficient of dry sand is approximately 0.20 W/(m.K) [15]. Since it is very complex to calculate the unsteady heat problem with a moving heat source, a simplification is made. A steady state is assumed, since the heated spot will move very slowly. Further a one dimensional heat conduction is assumed. The heated spot is then modelled as a small sphere (radius  $R = 0.01\text{m}$ ) with a constant temperature  $T_R$  of 1973.15K, and the surrounding sand is modelled as a bigger sphere (radius  $r = 0.15\text{m}$ ) with a constant temperature  $T_r$  of 300K at its outer surface. A representation of this is given in Figure 9.

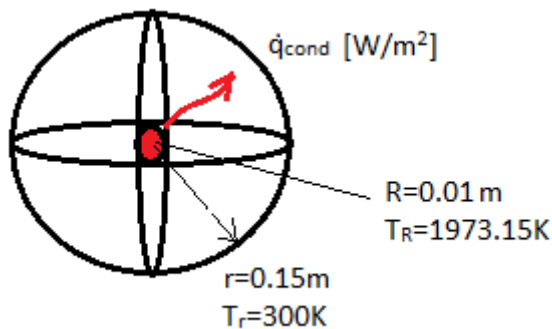


Figure 9: Representation of the simplified conduction problem.

The governing relation for the heat flow is then [18]:

$$q = (T_R - T_r) / (R^{-1} - r^{-1}) \cdot k \cdot 4\pi$$

This yields:  $q = 45\text{ W}$ . This is heat flow in all directions. Since we are heating a spot on a flat surface of sand, we lose only energy through conduction in downward direction. Therefore,  $q_{\text{cond}} = 0.5 q = 23\text{ W}$ .

*Note: Since the printing speed is not infinitely slow, a steady state assumption is not directly valid. Moving of the focal spot means a higher temperature gradient on the edge of the printed material, since the surrounding material will be colder. This implies a higher heat flow by conduction. Because it is assumed that the conduction loss is insignificant in comparison to the radiation loss, this is not further calculated due to time reasons.*

### 2.3.5 Convection

The heat transferred from a hot surface by natural convection is described by:

$$q_{\text{conv}} = h_c \cdot dT \cdot A,$$

where  $h_c$  is the convective heat transfer coefficient,  $dT$  the difference in temperature of the surface and the surroundings, and  $A$  the hot surface. The convective heat transfer coefficient for a horizontal hot plate is taken to be  $25 \text{ W/m}^2\text{K}$ , which seems to be a high estimate [15]. The temperature difference is  $1973.15\text{K}-300\text{K} = 1673.15\text{K}$ . With a circular hot surface with a radius of  $1\text{cm}$ , the area  $A$  equals  $\pi \cdot 10^{-4} \text{ m}^2$ . This yields a heat transfer  $q_{\text{conv}}$  of  $13\text{W}$ .

## 2.4 Incoming solar energy

### 2.4.1 Solar irradiation

The maximum daily solar irradiation per square meter depends on the global position and the local parameters such as clouds. The intensity of the sun light just outside the atmosphere equals  $1.353\text{kW/m}^2$ . Because this solar radiation has to pass the air mass of the atmosphere, the actual irradiation on the earth surface is lower, depending on the angle with the earth's normal surface. The air mass factor can be calculated with a formula proposed by Kasten and Young [19].

$$AM = (\cos(z) + 0.50572 \cdot (96.07995 - z)^{-1.6364})^{-1}$$

The angle of the solar irradiation with the earth's normal surface changes with the time on a day, and the season in a year. A sun path diagram for Eindhoven city is given in Figure 10. From this can be seen that the highest position of the sun is achieved in June around 13:45pm [20].

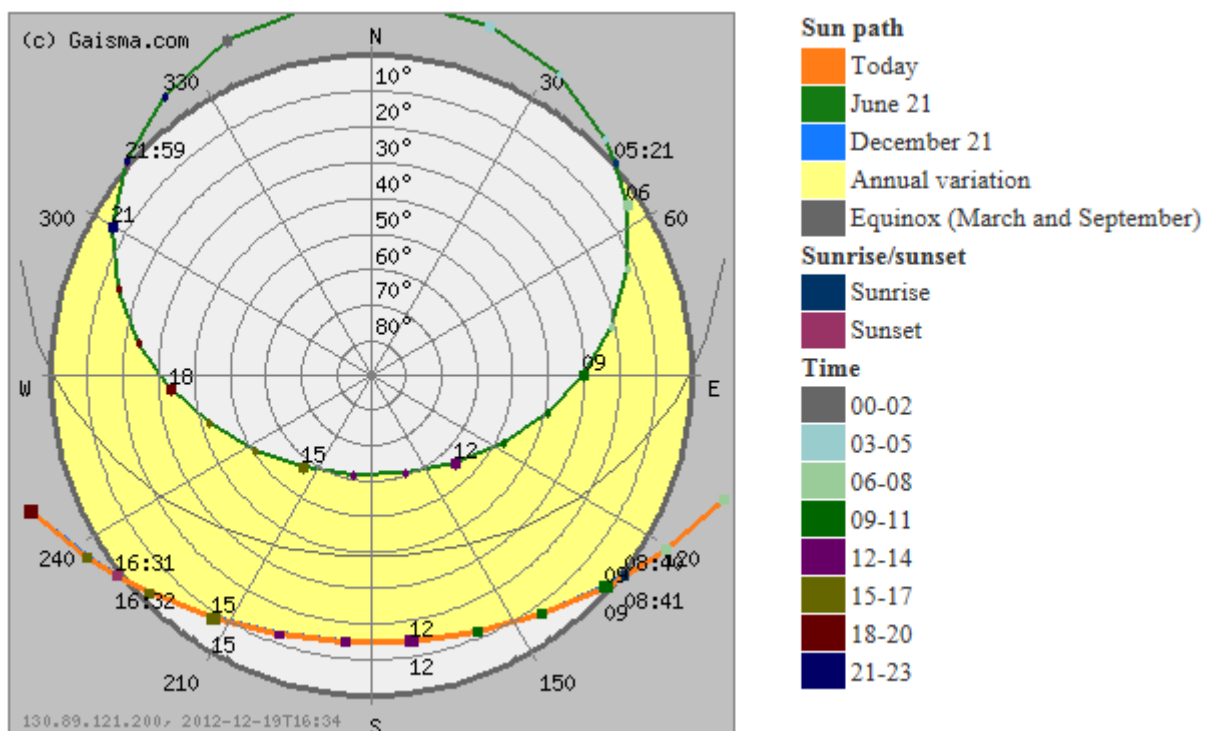


Figure 10: Sun path diagram for Eindhoven, the Netherlands. 'Today' = 19-12-2012 [20].

The angle of the sun is then approximately 60 degrees, which means that the angle of the sun with the earth's normal equals 40 degrees. This yields an AM factor of 1.3.

An approximate model for the solar intensity with non-polluted air as a function of the air mass is given by the equation [21]:

$$I_{\text{total}} = 1.1 \cdot I_0 \cdot 0.7^{(AM^{0.678})}$$

where  $I_0$  equals  $1.353\text{kW/m}^2$ , and the factor 1.1 accounts for 10% additional diffuse irradiation. This diffuse sunlight is not usable when focussing the sunlight with a lens, since only parallel rays are focussed in the focal spot. For this reason the useful incoming radiation on the lens  $q_{\text{lens}}$  equals  $I_{\text{total}}/1.1$ . This yields  $q_{\text{lens}} = 880\text{ W/m}^2$  during June in the Netherlands.

### 2.4.2 Lens efficiency

There are several types of Fresnel lenses offered on the internet. The type that is useful for solar applications is mostly made from PMMA and is UV-stabilised against ageing. Typical efficiencies range from 80% to 92% [22]. Solar lenses from eBay advertise with efficiencies of 83% - 85%. Assuming a safe 83% lens efficiency gives a  $\eta_{\text{lens}} = 0.83$ .

## 2.5 Energy balance and production rate

Since the incoming energy, the required energy and the energy losses are all known or reasonably estimated, the energy balance becomes:

$$q_{\text{lens}} \cdot \eta_{\text{lens}} \cdot \eta_{\text{reflection}} = q_{\text{rad}} + q_{\text{cond}} + q_{\text{conv}} + q_{\text{sand}},$$

where  $q_{\text{sand}}$  is the energy that goes into the sand for heating and melting. Solving this equation gives:  
 $880 \cdot 0.83 \cdot 0.6 = 205 + 23 + 13 + q_{\text{sand}}$

This yields  $q_{\text{sand}} = 197\text{W}$  per square meter of lens.

The rate of melting new sand onto an old layer is then defined as:

$Q_{\text{melt}} / (q_{\text{sand}} \cdot \eta_{\text{melt}})$  in  $[\text{time/kg}\cdot\text{m}^2]$ , which yields in the worst case scenario (melting pure silicon dioxide):

$$3270\text{KJ/kg} / (207\text{W/m}^2 \cdot 0.95) = 17473\text{ sec/kg}\cdot\text{m}^2 = 291\text{ min/kg}\cdot\text{m}^2,$$

and in the best case scenario (melting of regular soda-lime glass):

$$2814\text{KJ/kg} / (220\text{W/m}^2 \cdot 0.95) = 15036\text{ sec/kg}\cdot\text{m}^2 = 251\text{ min/kg}\cdot\text{m}^2.$$

## 2.6 Optimisation and lens choice

### 2.6.1 Lens choice

There are several Fresnel lenses offered on the internet. Within the category solar lenses (PMMA with UV-resistant coating), the choice of lens was mainly determined by the size and price. Efficiencies were equal or not mentioned. The chosen lens has dimensions of 1439 x 809 mm, and a focus of 1.1 m.

With a frame around the lens that overlaps the lens 4mm on all sides, the remaining surface becomes  $1.431 \cdot 0.801 = 1.15\text{ m}^2$ .

The calculated production rates of Chapter 2.5 are with this lens between 217 and 253 min/kg.

### 2.6.2 Optimisation

An overview of the energy flow in the sand printer is given in Figure 11. The sum of the pie chart is the total energy that falls on the lens surface.

## Energy flow sand printer

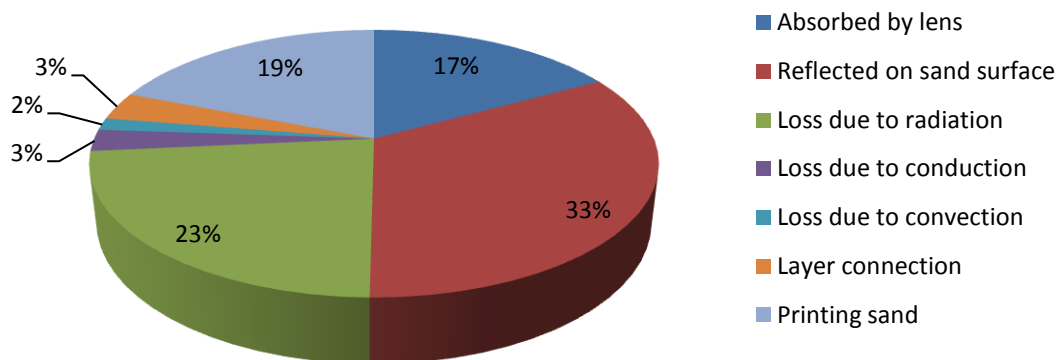


Figure 11: Energy flow in the sand printer

As can be seen, a relative large part of the incoming energy is reflected on the sand surface (33%), and radiated away from the hot surface (23%). To minimize these losses, two options are suggested:

- A heat resistant reflective shield around the printing spot, so that the radiated energy is reflected back on the print spot. The smoke that occurs due to chemical reactions of the organic impurities in the sand might affect the reflecting properties of the shield. This can be solved by adding a small fan, so the fumes are not deposited on the reflector.
- A small amount of graphite or carbon powder can be mixed with the sand to make it less reflective. The effect of this on the printed glass is unknown. Probably it will cause a darker colour of the end product and more chemical reactions with organic materials during the heating process, and thus more smoke.
- When the sun's position is closer to the horizon, the angle of the focal spot and the sand surface is very small. This causes additional reflection on the sand surface. To minimise this effect, a mirror can be added so that the focal spot hits the sand perpendicularly (See Figure 12). The printing surface can also be tilted towards the sun, so that the angle of irradiation is closer to 90 degrees.

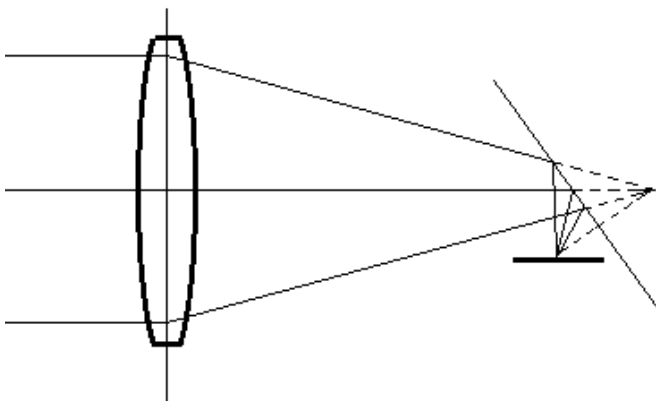


Figure 12: Schematic overview of added mirror to minimize reflections on the sand surface.

Due to time restrictions, none of these options are further investigated.

### 3 Designing

This chapter describes the process of designing the different aspects of the sand printer.

#### 3.1 Goal of design

The goal of the printer is very important on the design. For example, if the printer is designed to print houses, it might be wise not to move the printed product, but only the printing head. If the printer only makes small artefacts, it is easier to only move the product (on a table) and keep the whole lens and printing head fixed. Since the testing speed of the printer is about 4 hours per kg printed sand (see paragraph 2.6.1 2.6.1), only small products can be printed within reasonable time span. For this reason this project focuses on smaller objects. For example, these can be heat shields for furnaces, decorative art or sanitation devices.

#### 3.2 Choice of mechanical designs

Possible solutions for sand printing with a concentrated solar beam are summed up below. First the total design problems are divided three categories: *Concentrating the sun light*, *Moving the hot spot* and *Tracking the sun*. For each of the designing parts a list of possible solutions is given in Figure 13. Each solution is shortly discussed below, and then a conceptual design is made.

1. Concentrating sun light	2. Moving hot spot vs product	3. Tracking sun
a. Lens	a. Xyz table	a. Single axis tracker
b. Parabolic mirror	b. Mirror array	b. Dual axis tracker
c. Concave mirrors	c. Moving lens	

Figure 13: Morphologic overview of design

##### 3.2.1 Concentrating sun light

Concentrating the sun light to a small hot spot is essential to reach high temperatures. To achieve this, a lens can be used. Because a large area ( $\pm 1m^2$ ) of sun light must be captured, a glass lens is very heavy and expensive. A Fresnel lens is ideal because of its low weight and relatively low price. The focal distance of these lenses vary around 1 meter.



Figure 14: Fresnel lens [23]



Figure 15: Parabolic cooker [24]

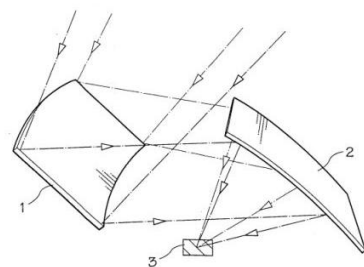


Figure 16: Concave mirror setup [25]

Another option is a parabolic mirror. These mirrors are widely used to cook food with sun light [24]. A disadvantage of this method is that the hot spot touches the printed product on the bottom side, and the product blocks the sunlight of the parabola. If a mirror is used to get the focal point behind the parabolic disk, at least half of the incident sunlight would be blocked by the back of this mirror. The used area of the parabola can be replaced by smaller separate mirrors; however this makes it hard to get a small focal area.

Instead of using a parabola and a mirror to get a down facing focal point, two concave mirrors can be used. This is option three, schematically displayed in Figure 16. The mirrors are only concave in one direction; therefore two mirrors are required to obtain a totally converged focal spot. The printed product is not blocking the incoming light in this setting. This option demands a complicated system for aiming the mirrors at the sun without moving the focal spot.

### 3.2.2 Moving hot spot versus product

The printed product has to move with respect to the focal point, so a three dimensional figure can be made. The first option is to use a xyz table, see Figure 17. This is very common for milling machines and 3d home build printers. An advantage of this system is that the software to operate it is relatively simple, and a lot of open source software is available. A disadvantage is that the linear guides may be sensitive to sand.

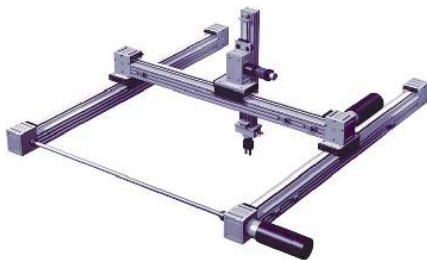


Figure 17: General purpose XYZ table [26]



Figure 18: Robotic fibre optic laser welding machine [27]

The second option is to move the hot spot with a mirror array. Instead of a mirror array, it is also possible to use a glass fibre cable to transport the laser light. This is very common with laser welding machines, since both the product and the laser are too heavy and large to move quickly. In order to use this type of moving system, the focused light of the sun needs to be diverged with a lens, in order to get a small parallel beam. At the end of the beam, another lens is required to focus the light again into a hot spot.

The last option is to move the whole lens. This might be an advantage if it can be coupled with the tracking system of the lens.

### 3.2.3 Tracking of the sun

The sun is moving along the horizon along a track that approximately fits in a plane. The angle of this plane with the earth's normal changes along the year, see Figure 19.

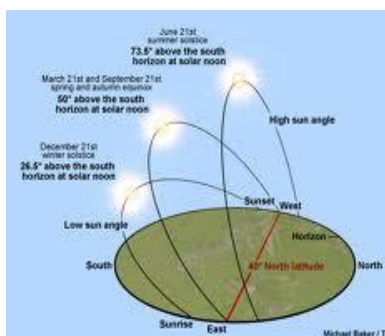


Figure 19: Solar trajectory

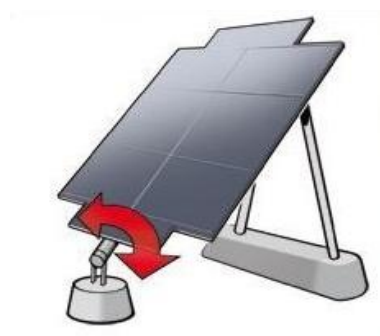


Figure 20: Single axis solar tracker

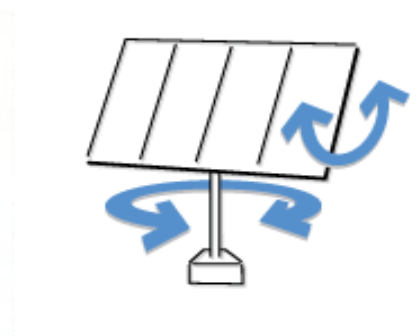


Figure 21: Dual axis solar tracker

This means that for one day the sun can be followed with only one actuator (See Figure 20). The variation of the sun along the year can manually be adjusted. This adjustment system is however quite complex, because the focal point of the lens system needs to remain on the same spot. Furthermore the location of the machine, the direction, and the season must be known for the initial setup before operation.

Another option is a dual axis sun tracker (See Figure 21). This option has two actuators. It can be operated with a timer or a light sensor.

### 3.3 Conceptual design

The best option for concentrating the solar light seems to be the Fresnel lens. From the given options it gives the smallest focal spot and the simplest mechanics to track the solar trajectory. A disadvantage is that the maximum area of the lens is around  $1\text{m}^2$ , since there are simply no bigger lenses for sale on the internet. This has probably to do with engineering constraints, as these lenses are injection moulded. If a larger area is required, a special lens design has to be made that is dividable in parts of around  $1\text{m}^2$ . For private individuals this might be an expensive option because of low ordering amounts and high tooling costs. According to Philips the price of bulk moulding of PMMA for solar concentrators will decrease to  $10\text{€} / \text{m}^2$  in the future [28].

For the movement of the hot spot a xyz table is chosen. This makes the driver software for printer the least complicated, since there is a separate control for the x, y and z direction. Furthermore it makes the printer compatible with existing open source software that converts 3d CAD models to machine code. This is regarded as a huge advantage.

For the tracking of the sun a dual axis tracker is preferred. This is mainly because the complexity of a dual and single axis tracker is approximately the same. The dual axis system uses two actuators for the two degrees, where the single axis system needs an actuator and a manually operated degree. Since the dual axis tracker does not need to be levelled, directed towards south, and manually adjusted to the location and season, this option is preferred.

The conceptual design for the 3d sand printer is given in Figure 22.

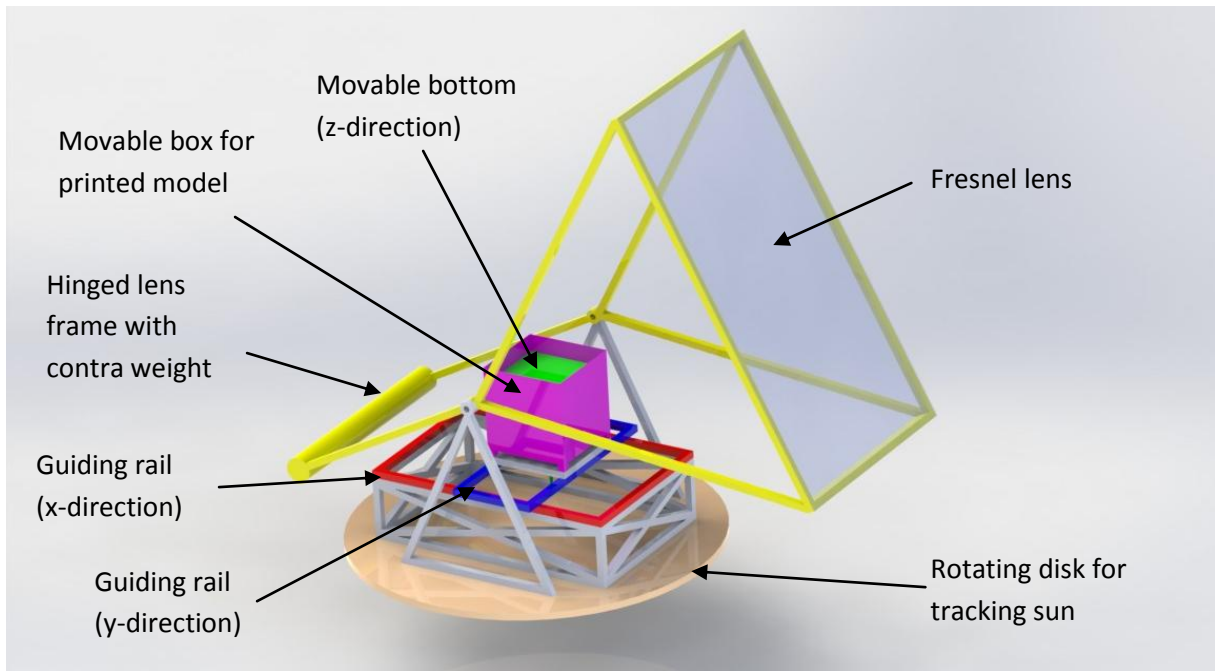


Figure 22: Conceptual design

The concept is detailed in Chapter 4.1.

### 3.4 Conceptual electrical drive system

There are several options to control the printer. A list is given below.

System	Pro	Con	Price *
1. Atmega controller	<ul style="list-style-type: none"> <li>- Low cost</li> <li>- Stand alone</li> </ul>	<ul style="list-style-type: none"> <li>- Lot of programming and research required</li> <li>- Difficult to convert CAD model to movements</li> </ul>	360 €
2. Prefabricated circuit board (e.g. Arduino / Raspberry Pi)	<ul style="list-style-type: none"> <li>- Low cost</li> <li>- Stand alone</li> </ul>	<ul style="list-style-type: none"> <li>- Intensive programming</li> <li>- Difficult to convert CAD model to movements</li> </ul>	390€
3. CNC control unit	<ul style="list-style-type: none"> <li>- Complete kit</li> <li>- Including powerful motors</li> </ul>	<ul style="list-style-type: none"> <li>- Unknown Chinese driver software</li> <li>- No adaption of driver software possible</li> <li>- Not USB compatible</li> </ul>	400€
4. Existing 3d printer kit	<ul style="list-style-type: none"> <li>- USB compatible</li> <li>- Open source firmware</li> <li>- Lots of software</li> </ul>	<ul style="list-style-type: none"> <li>- Expensive</li> <li>- Relatively small stepper motors (&lt;2A)</li> </ul>	450-600€

	and extensions available - No extensive programming required		
*Approximated, 5 motors á 50€/pc included.			

Figure 23: Overview of electronics

In order to drive the printer correctly, some non-standard printer/CNC operations must be executed. For example, adding a new layer of sand, or pausing when the sun intensity is too low. To do this, the code of the program needs to be changed according to these preferences, or the conversion of the CAD model to motor instructional code (mostly Gcode) needs to be accessed and altered. Option 3 drops out for that reason, since the software nor the Gcode is adaptable.

Since the time of the internship is limited (initially 3 months), it is not possible to write a total code for the printer next to building the hardware. For that reason the relative expensive option of an existing electronics kit is chosen to drive the sand printer. It is possible to modify the included driver software to customised needs, but probably this will not be necessary since there are several settings that can be changed in the existing firmware. In the open source software (e.g. ReplicatorG) a CAD model can be imported as .STL file and converted to a print trajectory in Gcode.

Finally the MakerBot Gen 4 Electronics kit is acquired. This kit has the most powerful stepper motor drivers, so it can drive motors with a current up to 2.8 A with a maximum torque of 0.45Nm.

# 4 Construction of design

## 4.1 Refining concept

The concept given in the previous chapter evolved with an iterative process according to the drawings in Figure 24 -Figure 26.

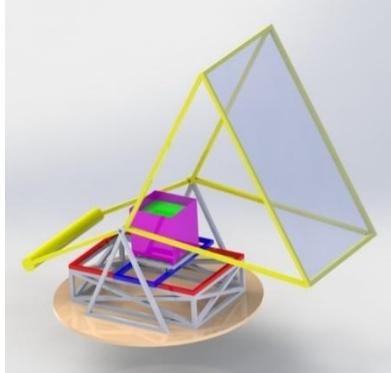


Figure 24: Initial concept



Figure 25: Intermediate design 1



Figure 26: Intermediate design 2

A few key concepts of the final design are mentioned in Figure 27 and explained below.

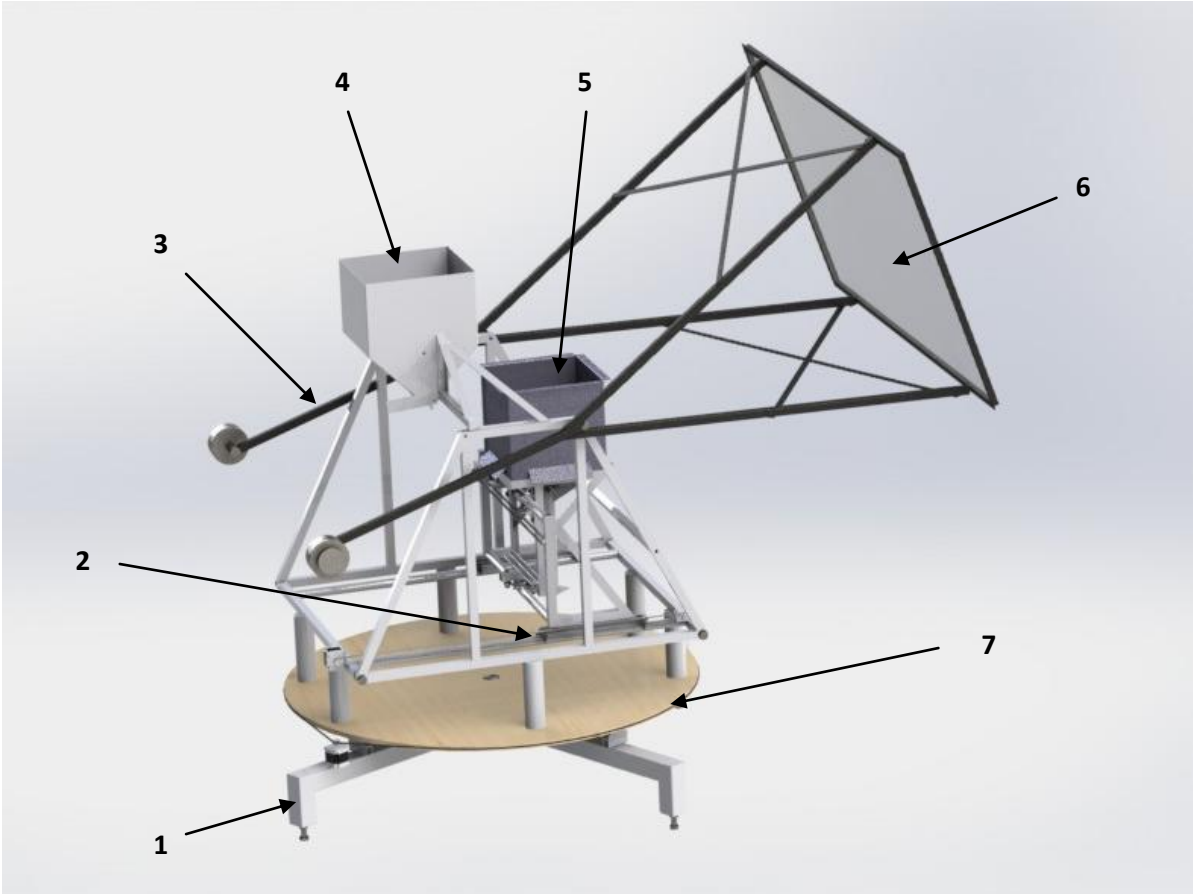


Figure 27: Final design (December 2012)

## 1. Adjustable legs

Because the wooden disk which supports the rails is flexible, there are four legs. They support the disk with four castor wheels (Figure 28). To avoid imbalance and to level the machine, each support is equipped with an adjustable M16 bolt.

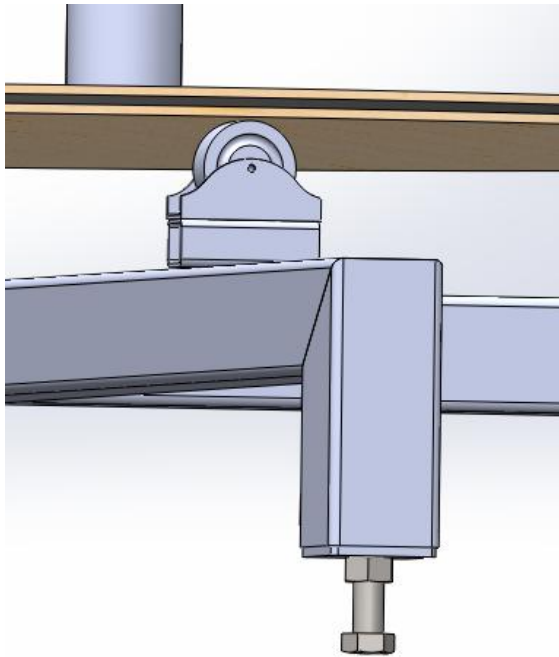


Figure 28: CAD model of support



Figure 29: Constructed support in workshop of WOT

## 2. XY rail

For the rail system a simple system of bearings on a galvanised pipe is used which is schematically represented in Figure 30. This is a relatively cheap construction, and sand will not interfere with the rollers, since it will simply fall off the tube.

The lowest rail system (X-direction) is over constrained because there are four units as given in Figure 31 on two rails. This is however not a problem, since the distance between the rails is accurate within one mm. This will lift the moving train with maximal 1 mm, since the wheels are touching the tube with an angle of 45 degrees with the horizontal.

The upper rail system is designed without being over constrained. The roller bearings that prevent lifting of the top unit have a free play of approximately 1 mm. The assembly is given in Figure 32.

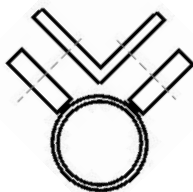


Figure 30: Schematic rail

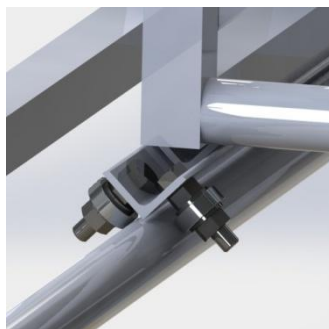


Figure 31: CAD model of rail

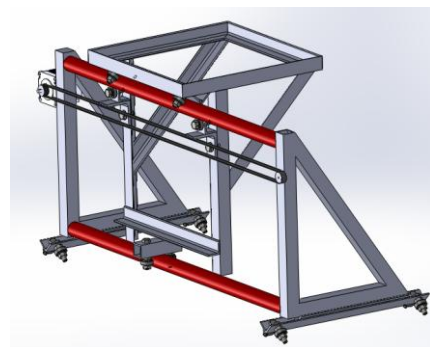


Figure 32: CAD model of X and Y train

### 3. Balanced lens frame

The lens frame is almost balanced with contra weights so that there is no strong motor required to move the system. To prevent free play in the system, the contra weights are slightly lighter than the lens, so when the lens is actuated the sign of the load on the actuator does never change. The actuation is done with a stepper motor with a spindle. The focal point of the lens is located exactly between the two hinge supports. When the lens is tilted towards the sun, the focal point remains on the same place.

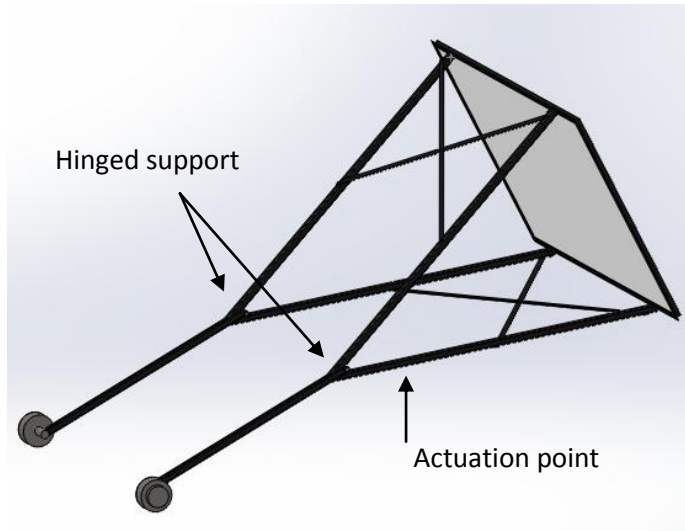


Figure 33: Balanced lens frame

### 4. Automated sand filler

The unit that fills the sand in the print box is given in Figure 34.

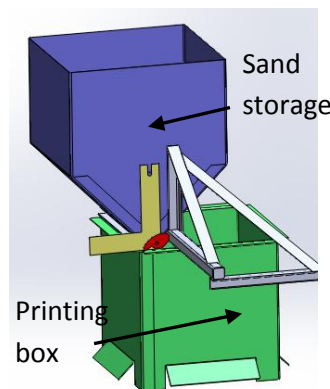


Figure 34: Filling system

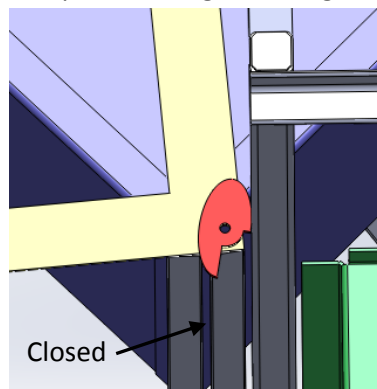


Figure 35: Closed filling mechanism

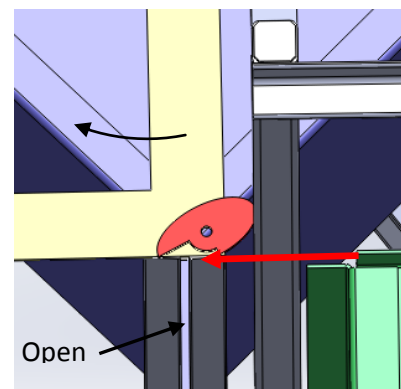


Figure 36: Open filling mechanism

The green box can move on the rails under the focal spot. The sand on the surface of the box will be printed when the focal spot touches it. After each printed layer, a new layer of sand has to be added in the printing box. This happens when the printing box is moved under the storage box. The edge of the printing box will push against a small lever (red in Figure 35) so it opens the valve of the storage box. Sand will fall out until it reaches the valve. When the printing box moves further, a neat layer of new sand is positioned on top. When it moves even further, the valve will close itself by gravity. When the box moves backwards, it will not open the valve again because of the shape of the lever. The storage box is made from galvanised sheet metal 0f 0.75mm thickness.

A prototype of the sand filler is made to ensure that the valve operation would work correctly (See Figure 37). This yielded useful insights.

- Every moving part must have free play of approximately 2 mm at least to prevent extreme friction caused by the sand.
- Larger openings (up to 5mm) in the closing system are not a big problem, if the sand is allowed to heap up after the opening it will block further sand to flow.
- A tiny opening facing downwards will drain a lot of sand like an hour glass. A small example of this is the volume marked with 1 in Figure 38. This small amount was drained before the valve was open.
- The dead volume of the closing mechanism will cause a relatively high amount of sand to drop out after closing. This is the sand marked with 3 in Figure 38. This dead volume is minimised in the final design by minimising the distance between valve and sand bed.
- The desired deposited volume (marked with 2) has rounded corners just after the opening. This is also caused by the distance between the sand bed and valve.



Figure 37: Wooden prototype of sand filler

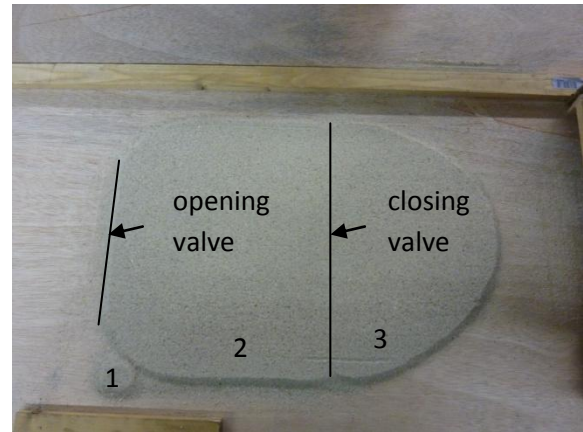


Figure 38: Deposited sand

## 5. Print box with movable bottom

The printing box (green) has a sliding bottom. There is only one motor with spindle to drive this z-movement. An overview of this is given in Figure 39. The sand box has openings on the bottom, so that when the bottom is at its most downward position, the loose sand will fall out automatically. This makes it easier to move the bottom upwards when the printing is done. The printing box is made from sheet metal of 2 mm thickness.

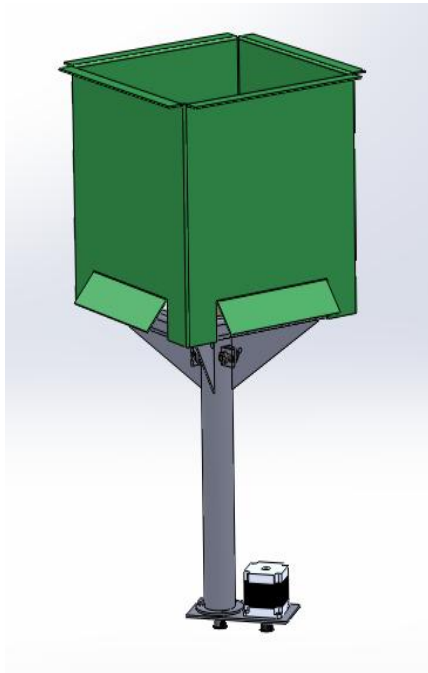


Figure 39: Print box

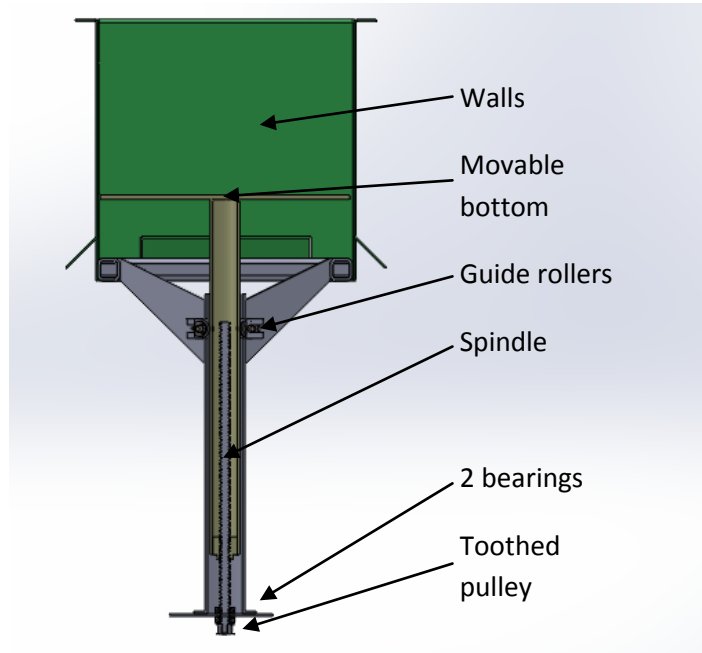


Figure 40: Cross section of print box

## 6. Fresnel lens

The Fresnel lens is acquired from the company Shenzhen HaiWang Sensor Co.,Ltd [23]. It is made from PMMA with a UV coating to minimise degradation caused by sun light. The focal distance is 1.1 meter. It is supported in a frame made out of T-beams, so that the frame only overlaps the lens 4mm on each side. The lens is glued to the frame with silicone. The good connection between lens and frame is necessary because the lens makes the lens frame rigid. By using silicone glue, excess stresses due to different expansion rates from the frame and lens are avoided.

## 7. Rotating disk

The disk under the printer is used to rotate the whole assembly towards the sun. It is supported by a ball bearing in the middle, and four wheels on each of the legs to prevent excess deformation (See Figure 41). Although the disk has 5 supports this way and is thus over constrained, it still touches all four wheels due to its flexible nature.

It is made from wood, and a small slot for a timing belt is made in the side. A small stepper motor with a transmission of 4:1 (approximately 1.5 Nm on output shaft) and a pulley of 16mm is used to drive it. This is enough to overcome the friction of the bearing and wheels, even when an adult person is sitting on the disk.

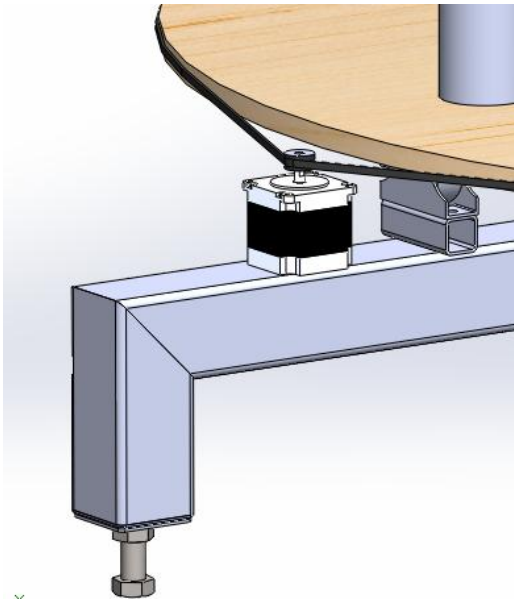


Figure 41: Support and disc actuator

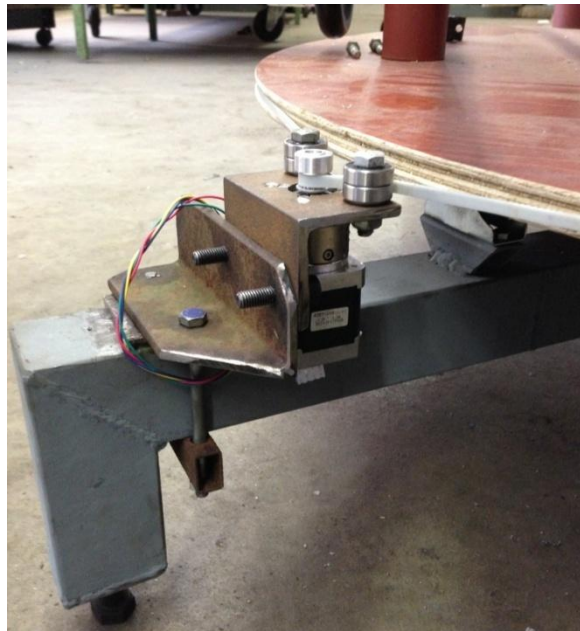


Figure 42: Built model of disc and actuator

## 4.2 Calculating bearing loads and rail thickness

### Top linear bearings

The printable volume of 0.3 x 0.3 x 0.3 m has a filled weight of approximately 40 kg and rests on one bar that acts as a linear guide (See Figure 43). Four bearings suspend the whole weight of the sand and the moving structure. The total moving weight is approximated at 55 kg. All four of the bearings are equally loaded. Since the bearings are under an angle of 45 degrees, this yields a radial force of  $55 \cdot 9.8 / (4 \cdot 0.5 \cdot \sqrt{2}) = 191 \text{ N}$  on each of the bearings.

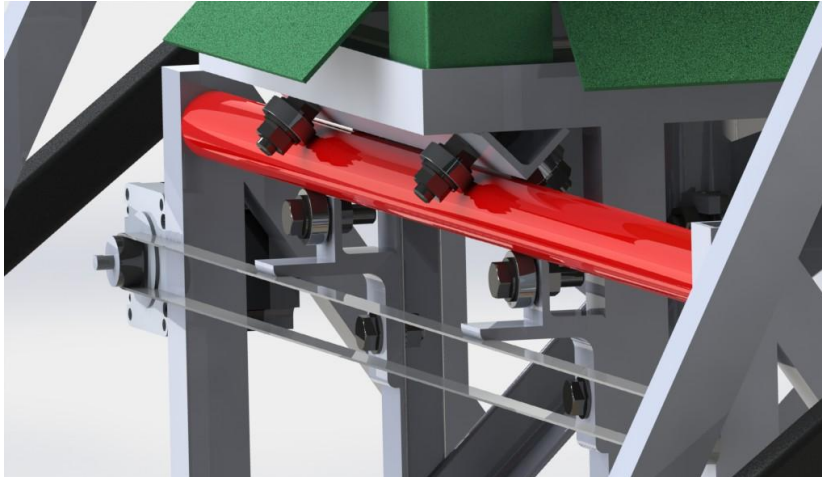


Figure 43: Top linear bearing

The chosen bearings are of the type 608, with an outer diameter of 22 and axis opening of 8 mm. This is the type that is widely used in skating, so they are offered on the internet at 10 times a lower price than the regular bearing companies. The maximal loads for the official bearings are 330 kg and 135 kg dynamic and static respectively. The Chinese skate bearings are probably made lower quality, but can still handle the requested loads.

### Top linear guiding

For the guiding rail a galvanised gas pipe is chosen. In the worst case, the loading on the frame is regarded as a point load in the middle of the guiding (See Figure 44). This would simulate the situation when the sand box is accelerated with a high speed, so all the load rests only on two of the rollers.

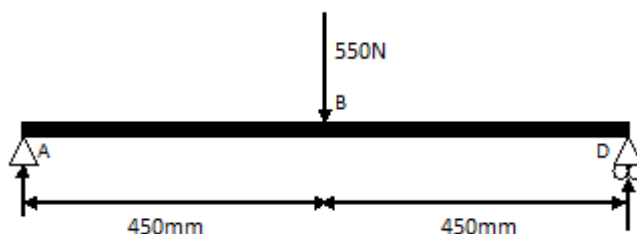


Figure 44: Schematic visualisation of top rail with point load

The following formulas are used to calculate the maximum displacement in the middle of the beam. First the second moment of area is calculated for a 3/4" gas pipe:

$$I = \pi (d_o^4 - d_i^4) / 64 = 1.67e-8,$$

where  $d_o$  is the outer diameter (26.9mm), and  $d_i$  the inner diameter of the profile section.

The maximal deflection in the middle is then represented by:

$$w = 1/48 * F * l^3 / (E * I), \quad \text{which yields } w = 2.4 \text{ mm},$$

where  $F$  is the force in Newton,  $l$  the total length of the profile and  $E$  the Young's modulus of elasticity (210Gpa).

A total deflection of 2.4 mm is quite high, but in reality this will be lower. The rail beam is clamped at the two ends, and not only hinge supported, and the load is not centred in the middle, but spread over two points with a distance of 300mm. For this reason this deflection is not further calculated.

### **Bottom linear guide**

The same pipe (3/4" gas pipe) is used for the bottom rail. This rail is longer, and will yield a higher deflection in the middle. This is not a problem, since this rail can easily be supported in the middle if required.

## **4.3 Calculating required motor force/choosing motors**

There are five degrees that needs to be actuated.

- two axis to track the sun with the lens
- three linear movements for the xyz table

In the paragraphs below the required forces are calculated per motor.

### **4.3.1 Sun tracking (rotation of table)**

To direct the whole table in the direction of the sun a geared stepper motor is used. A test with a stepper motor (2A phase current, 0.45Nm rated torque) yielded that this could approximately do the job, but with some disturbances (a push against the machine for example) the motor lost track. The stepper motor was then not able to get out of the electrical slipping state. For this reason a motor with a reduction box of 4:1 is chosen. The new motor has no problem with loosing track.

The same motor is chosen to actuate the spindle to rotate the lens. This motor is sufficient, since the lens frame is almost balanced, and the motor only needs to accelerate the system. Since this can be a very low acceleration (the sun does not move so quickly), there is not much strain on the motor force.

### **4.3.2 Z-movement**

The z-movement is the movement that requires the most force. It has to press the bottom of the sand box up- and downwards and overcome the friction. The moving bottom with the maximum amount of sand has an estimated weight of 45 kg.

The friction caused by the sand on the walls of the box is roughly calculated using super positioning two phenomena.

The first one is the static friction when the sand is not moved. This is done using the general friction formula:  $F_{\text{normal}} \cdot \mu_{\text{static}} = F_{\text{friction}}$ . These calculations can be found in paragraph 4.3.2.1.

The second phenomenon occurs when moving the bottom of the box upwards. Sand slides along a natural slope, which makes that some parts of the sand will act as a wedge, clamping between the walls and the natural sliding surface. This will convert a fraction of the upward force into a friction force. These calculations can be found in paragraph 4.3.2.2.

The last part of the friction that needs to be superposed to achieve the required motor force is the friction in the drive system. This can be found in paragraph 4.3.2.3.

The force that is required to accelerate the whole sand upwards is neglected. The required speed is very low, 1cm in 5 seconds = 0.002m/s is enough. When the motor accelerates to this velocity in 1/5 of a second, this equals an acceleration of 0.01m/s<sup>2</sup>. Multiplied with the total moving weight of 45 kg, this yields a force of less than half a Newton.

The friction that occurs when moving downwards can also be neglected, since the sand will not be compressed. If it will exert a friction force on the walls, this means that the density will locally decrease, resulting in falling sand and not in a noticeable friction.

#### 4.3.2.1 Static friction

##### Minimal case

The minimal case of static friction occurs when sand is not compressed and not vibrated. In this case the sand will slide along its natural slope, also known as angle of repose. This angle is 30 degrees for dry sand. This means that a pyramid of sand on the bottom remains, even when the walls would not exist. A simplified picture is given in Figure 45.

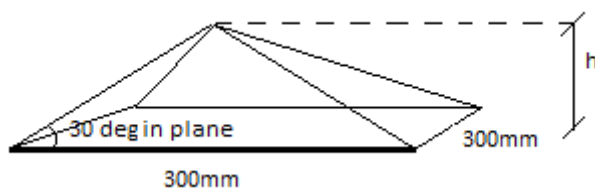


Figure 45: Simplified representation of sand on a square plate

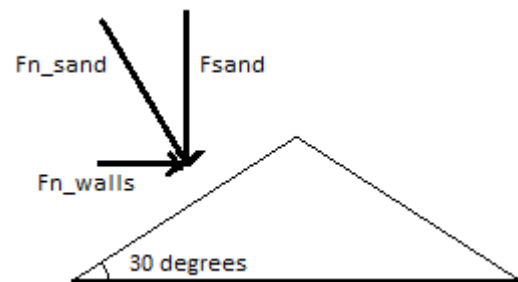


Figure 46: VLS of sliding sand

The sand above the pyramid in the printing box will cause the friction with the walls. This is in the filled case: Total Volume-volume of pyramid = (width\*height\*length) - (1/3\*bottom surface of pyramid\*height of pyramid). This yields:  $0.3^3 - 1/3 \cdot 0.3^2 \cdot (0.5 \cdot 0.3 \cdot \tan(34)) = 24.0$  Litre.

This volume with a mass of 34.6 kg slides over a slope of 30 degrees against the walls, represented in Figure 46.

The normal force  $F_{n\_walls}$  exerted by the walls on the sand is in this case calculated with:  
 $mass\_sand \cdot g / \tan(60) = 345 / \tan(90-34) = 228.4$  Newton.

The friction coefficient of concrete on steel is 0.45 [29]. This is estimated to be the same as with sand on steel. This yields a friction force of  $228.4 \cdot 0.45 = 103\text{N}$ .

**Maximal case**

This calculation is valid when the sand is treated as a fluid. When excited fast enough vibration, sand will behave slightly like a fluid; the natural slope will approach 0 degrees. The friction between the sand grains can be neglected in this case.

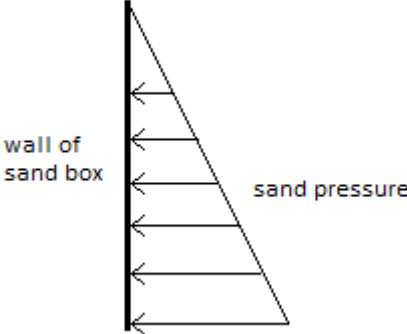


Figure 47: Pressure of sand when treated as fluid

When the sand box is filled for the total 300mm of depth, the pressure is calculated as:  $P = \rho \cdot h \cdot g$ , where  $\rho$  is the density of sand ( $1442\text{kg/m}^3$ ),  $h$  the height (300mm) and  $g$  the gravity constant.

The pressure at the bottom of the walls is then calculated to be 4326Pa. Since the pressure is assumed to increase linear with the height, the average pressure is  $4326/2 = 2126$  Pa. The net normal force on the four walls is then:  $4 \cdot 2126 \cdot 0.3^2 = 778.68\text{N}$ .

Multiplying the net normal force with the friction coefficient, a total friction of 350N is calculated, assuming fluidal behaviour of the sand. This is almost 3.5 times higher than the previous minimal calculations. This result ( $F_{\text{friction\_static}} = 350\text{N}$ ) is therefore used as a safe estimation in further calculations.

**4.3.2.2 Friction due to sliding mechanisms in the sand during movement.**

When pressed upwards, another phenomenon occurs aside to the static friction. The sand tends to clamp itself between the static bottom pyramid and the walls as a wedge. A 2 dimensional simplification of this process is given in Figure 48.

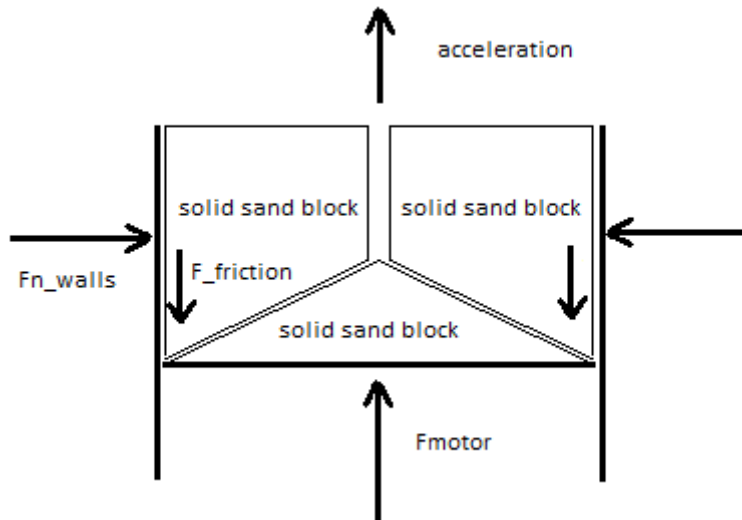


Figure 48: Wedging effect of sand

The forces of friction are enlarged when the motor moves the platform upwards. This induced friction force equals:  $F_{fr\_induced} = F_{n\_induced} * \mu = F_{motor} * (0.45/\tan(56)) = F_{motor} * 0.30$ . This means that we need a motor force that is 30% higher than we would need without this induced friction. So we set  $\eta_{friction\_induced} = 0.70$ .

#### 4.3.2.3 Friction in the drive system

The friction in the drive system is assumed to be more or less linear with the motor speed, since it consists mainly of a lubricated spindle. The efficiency of a typical trapezoidal spindle is around 0.5. A simple test setup with the spindle at hand (derived from a car jack) yielded the ratio input power: output power equals to 1: 0.17, so we set  $\eta_{drive}=0.17$ .

#### 4.3.2.4 Total force required for z-stage and choice of motor

Summing all the forces and efficiencies, the following formula for the required minimal force on the bottom of the sand box is solved.

$$F_{z\_spindle\_out} = (\eta_{friction\_induced})^{-1} * (F_{friction\_static} + F_g = 1/0.70 * (350 + 45 * 9.8)) = 1130N$$

For the transmission from motor to z-movement a spindle is used. This spindle has a pitch of 2.5 mm and is direct driven by a planetary geared stepper motor. The relation between the moment of the motor and the force in z-direction of the spindle is then:

$$M_{spindle} * 2\pi/pitch * \eta_{drive} = F_{z\_spindle\_out} = M * 2\pi/2.5e-3 * 0.17 = 1130 N.$$

The ingoing moment on the spindle is then calculated to be **2.64 Nm**.

The choice for the motor in Z-direction is a Nema 17 sized stepper motor. This motor can yield 0.35Nm with a current of 1.8A. This is the maximum size that the acquired motor driver can handle without additional cooling. To yield a higher torque, a reduction box is selected. A reasonable priced gearbox was found with a reduction ratio of 12:1. With a gearbox efficiency of 80% a total torque on the outgoing shaft of 3.36Nm is reached, which is sufficient.

### 4.3.3 XY- movement

In order to calculate the size of the motor for the X and Y movements (in horizontal plane), three forces are calculated. The first one is the force that is required to overcome the rolling resistance. This is the resistance that occurs when a cylinder is rolled over a flat surface. The second one is the force that is required to overcome the friction in the bearings. The last one is the force to get a reasonable acceleration for the unit.

Since the two linear guiding systems are not so much different, only the lowest one is calculated. This is the one with the most weight on it, and thus the largest forces. A matching motor is selected to drive this movement. The motor for the upper linear guide is chosen the same for simplicity reasons.

#### 4.3.3.1 Rolling resistance

For the rolling resistance the following formula is valid:

$$F = f \times W/R,$$

where:

F = the force in [N] acting in the centre of the cylinder in the direction of the motion,

f = the coefficient of rolling friction in [m], for steel on steel in the range of 0.0005m [29].

W = the force in N pressing the cylinder on the flat disk,

R = the diameter of the cylinder, 22e-3 in this case.

The force W that presses each of the eight wheels on the guide rails is equal to:

$$W = 60 \times 9.8 / 8 / \sqrt{2} = 52\text{N},$$

where the root factor comes from the fact that the wheels are placed under an angle of 45 degrees.

The friction force due to the rolling resistance of the metal bearings on the metal guide rails equals:

$$F = 5e-4 \times 52 / 22e-3 = 1.18 \text{ N per wheel. In total this is } 9.5\text{N}.$$

#### 4.3.3.2 Roller bearing friction

The following formula for the bearing friction can be used [29]:

$$F_{\text{bearing}} = F_{\text{radial}} \times f \times (d/2) / (D/2) \times n,$$

with

$F_{\text{radial}}$  = the radial force on the bearing (52N, see before)

f = the coefficient of friction of rolling bearing (0.0025 for radial loaded single row ball bearings with seals)

d = the shaft diameter of the bearing (8 mm)

D = the outer diameter of the bearing

n = the start up factor, maximal 2.

The roller bearing friction force  $F_{\text{bearing}}$  becomes then:  $52\text{N} \times 25e-4 \times 4e-3 / 11e-3 \times 2 = 0.1\text{N}$ . For all eight wheels this becomes 0.8N.

#### 4.3.3.3 Acceleration

The total weight of the moving Y-table is 60 kg. When the whole Y-table is moving with 0.05m/s, the motor should be able to stop it within 1mm for an accurate print trajectory. With a linear deceleration the time of the stopping equals  $(1e-3/5e-2)*2 = 4/100$  sec. The deceleration equals then  $0.05m/s / 4e-2s = 1.25m/s^2$ . The required force for this is:  $60kg * 1.25m/s^2 = 75N$ .

#### 4.3.3.4 Choice of motor

The total motor force needs to be the sum of the above mentioned forces, multiplied by a factor to deal with the efficiency of the drive train. This factor is set to  $0.8^{-1}$ , and covers the losses of the timing belt. The total force is then equal to  $(9.5 + 0.8 + 75) * 0.8^{-1} = 107N$ . With a pulley diameter of 16mm, this equals a torque of 0.86Nm.

The motor that is chosen is again a Nema 17 sized stepper motor with a gearbox of 4:1. This motor can yield approximately 1.1 Nm, which is sufficient.

### 4.4 Installation of electronics board

To drive the motors for the printer, the MakerBot gen 4 electronics kit is acquired. To obtain access to the source code of the firmware, the new open source firmware Sailfish is installed. The main things to change in the firmware are:

- A waiting command when the sun intensity is too low.
- A standard movement after each finished layer to move the printing box under the filler before printing a new layer.

After a couple of days trying, it turned out to be too complicated to change these things in the code. To achieve the same results, it is also possible to use the existing software in a smart way. A thermocouple is normally attached to the circuit board that runs the printer extruder of the MakerBot. In the open source software, the Gcode is accessible. Here a waiting command can be given to wait until the thermocouple has reached a certain temperature. This thermocouple is replaced by a pyranometer, which contains also a thermocouple. The temperature that the software is reading now, is a measurement of the intensity level of the sun. This intensity has a good relation with the printing speed. Under a certain 'temperature' the printer is ordered to stop.

The standard movement for the filling of sand is also implemented in the Gcode. After each z-movement, a line of code is implemented that orders the printing box to move first under the filler before going on with printing the following layer.

These changes in the Gcode can be done manually, but in the future a C-file can be written. The process of putting a model in the sand printer can then become:

- saving a cad file as .STL-file
- convert the .STL-file in the printer software (e.g. ReplicatorG) to Gcode
- modify the created Gcode with a C-executable to build in wait commands and filling commands
- upload the modified Gcode to the printer and run.

#### 4.4.1 Sun tracking

The dual axis sun tracking is done with a separate Arduino board. This is because it is easier to program a separate Arduino than to modify the software of the printer electronics. For each movement two light sensors are mounted with an angle of approximately 90 degrees. These sensor values are captured with the Arduino board. A smart program written by a WOT member reads which sensor captures most of the light and rotates the motor in that direction until both sensors receive an equal amount of sun light.

## 4.5 Building of concept

Some pictures are given for a small impression of the building process. The building of the design is not yet finished, as can be seen from the pictures.



Figure 49: Welding of lens assembly



Figure 50: Welding of lens frame from T-profile

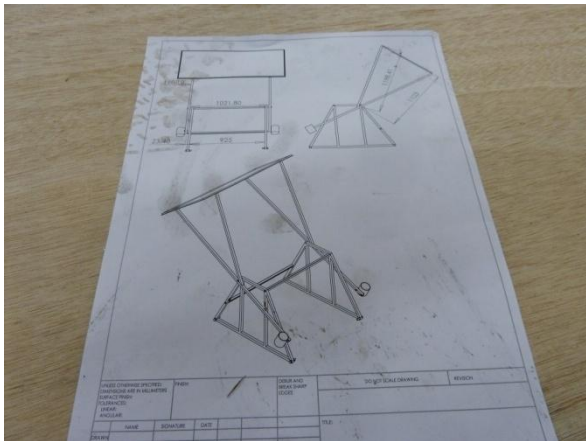


Figure 51: Drawing of lens assembly



Figure 52: Corner of lens frame; less than 4mm overlap

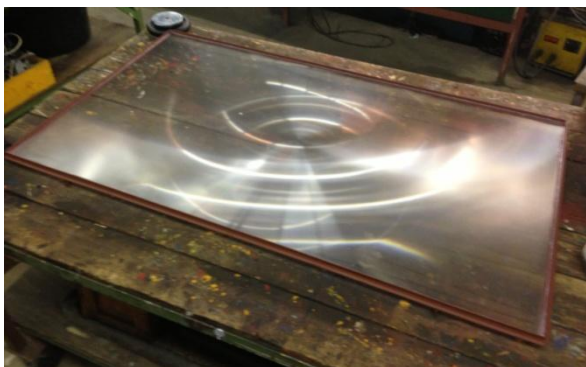


Figure 53: Beautiful pattern in Fresnel lens



Figure 54: Temporary assembly with frame clamps



Figure 55: Assembly of main frame



Figure 56: Temporary assembly of lens frame

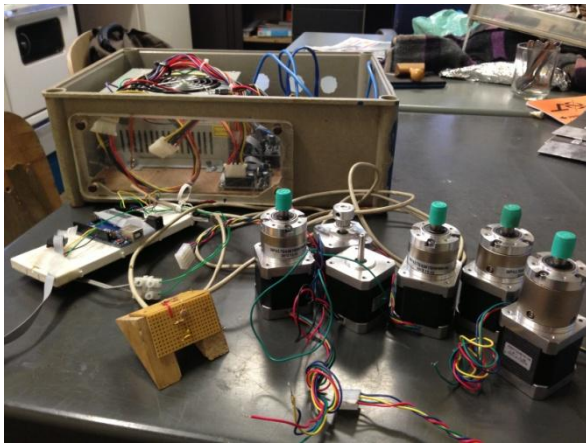


Figure 57: Electronics and motors with planetary gearboxes



Figure 58: Motor without gearbox: too weak

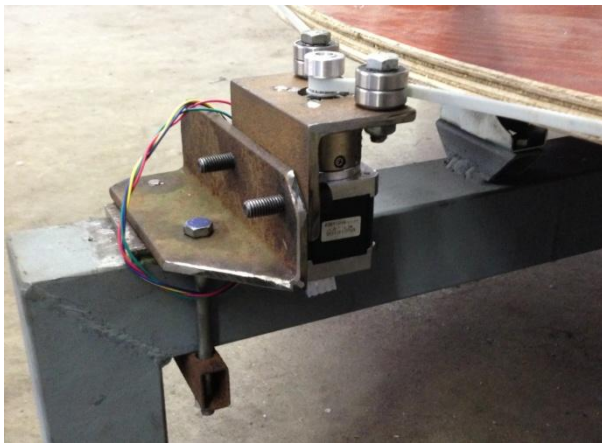


Figure 59: Improved assembly: motor with gearbox 4:1



Figure 60: MakerBot Gen 4 Electronics kit, nicely in box



Figure 61: Assembly without lens



Figure 62: Assembly with lens

## 5 Conclusion and recommendations

The concept of printing sand with solar energy impresses the imagination. Especially for countries with a high amount of solar irradiation and freely available sand, this way of prototyping and constructing might be an interesting start of entrepreneurship. For a lot of developing countries around the equator this is the case. The printing rates are however relatively slow, so only small products can be made in a reasonable time span. Depending on the material properties of the printed products, several things can be constructed. The material properties such as strength, heat resistance and surface appearance are not yet tested however.

The price of the machine is higher than estimated in the beginning, mainly due to higher costs of the lens. The lens was ordered from China, but after the order another amount had to be paid for additional fees of transport, and import fees at the Dutch border. Also the electronics were more expensive than expected. This is mainly because the choice is made for an all inclusive prefabricated set of electronics. A few cost reductions can be made by smart shipments and importing of goods at the border and cheaper electronics. The Fresnel lens can be cut into four parts for example, reducing the costs by more than 150 USD, without losing much of the performance. With a cheaper electronic kit, such as the Sanguinololu, the price can lower again with an estimated 200 USD. The total price of the printer will then decrease to an estimated 1000 Euro, which is still a high investment for entrepreneurs in developing countries. This depends of course on the market for the products, and the rate of return, which are currently unknown.

The machine that is being created at the WOT at during this internship needs to be finished before a product can be printed. The four months that were assigned for this internship turned out to be too optimistic to finish the whole machine. The things that need to be done are listed below.

- Building of print box
- Building of sand filler system
- Fitting motors and timing belts for x and y movement
- Fitting motor and spindle for lens movement (up-down)
- Putting all electronics together on machine with extended wiring
- Testing the machine in summer

The expectation is that with the help of volunteers at the WOT, the machine will be ready to print before summer 2013.

### 5.1 Recommendations

A few recommendations on improvement of the design can be made. Some of them were too time extensive to implement during the internship, and some of them were revealed during the assembly.

- Changing the firmware of the printer to relate the printing speed to the reached temperature of the printing spot.
  - o The current printing program does not take the temperature of the melting spot into account. The machine waits till the solar intensity comes above a certain threshold, then it starts to wait for a set amount of time to heat up the sand in the focal spot. After this time (approximated 30 sec) it starts to print with a constant velocity. Assumed is then that with this certain solar intensity, the sand is melting. When the sun intensity is too low, the printer finishes its current Gcode command line (1 cm in

the printed piece at most), before it will wait again for the solar threshold. In the current software there is no relation between the actual temperature of the printed sand and the printing velocity. Also the phenomenon of heating up of the sand is not included in the software.

- Belt tensioning system for rotating disk
  - The belt of the rotating disk needs a tensioning system. Probably due to temperature differences, the belt becomes loose or very tight after a couple of days when it was firstly tensioned correctly.
- Replacement of disk supporting wheels with hard wheels.
  - The wheels that support the disk have a soft rubber layer. The initial thought was that this would prevent damage to the wooden disk, and would run smoother than hard wheels. After a couple of days without moving the disk, the wheels are slightly flattened by the continuous pressure. This makes that the disk is not rotating with a smooth movement at all.

## 6 Sources

- [1] M. Kayser, SolarSinter Project, [www.markuskayser.com](http://www.markuskayser.com), visited: 22-07-2012.
- [2] D\_shape, The 21st century revolution in building technology, [d-shape.com](http://d-shape.com), visited: 22-07-2012.
- [3] B. Khoshnevis, Contour Crafting, <http://www.contourcrafting.org/>, visited: 21-07-2012.
- [4] Unknown, Zand uit alle windstreken, [www.kijkeensomlaag.nl](http://www.kijkeensomlaag.nl), visited 1-10-2011.
- [5] A. Fluegel, "Modeling of glass liquidus temperatures using disconnected peak functions," in *ACerS 2007 Glass and Optical Materials Division Meeting*, Rochester, 2007.
- [6] M. Janssens, Zand, [www.geologievannederland.nl](http://www.geologievannederland.nl), 2011.
- [7] W. Deer, A. Howie and J. Zussman, in *An Introduction to the Rock Forming Minerals*, ISBN 0-582-44210-9, Logman, 1966, pp. 340-355.
- [8] D. Brems, P. Degryse, F. Hasendoncks, D. Gimeno, A. Silvestri, E. Vassilieva, S. Luypaers and J. Honings, "Western Mediterranean sand deposits as a raw material for Roman glass production," *Journal of Archaeological Science*, no. 39, pp. 2897-2907, 2012.
- [9] C. Linke, O. Möhler, A. Veres, A. Mohacsi, Z. Bozóki, G. Szabo and M. Schnaiter, "Optical properties and mineralogical composition of different Saharan mineral dust samples: a laboratory study," *Atmospheric Chemistry and Physics*, no. 6, pp. 3315-3323, 2006.
- [10] EcoGlass, Software KMEN for glass properties calculation, Jablonec nad Nisou: [www.ecoglass-optic.com](http://www.ecoglass-optic.com), 2009.
- [11] H. Yamamoto, Glass Properties Estimation program, [Pirika.com](http://Pirika.com), 2012.
- [12] O. V. Mazurin, The SciGlass database 6.6, [www.scienceserve.com/Software/SciGlass/](http://www.scienceserve.com/Software/SciGlass/).
- [13] A. Fluegel, "Glass viscosity calculation based on a global statistical modelling approach," *Glass Technology: European Journal of Glass Science and Technology*, vol. 48, no. 1, p. Part A, 2007.
- [14] S. Plum, P. Graf, M. Beckers, J. Boersma, E. Van den Dungen, M. Frijns and F. Verbakel, "Advanced heating techniques for glass melting," Technische Universiteit Eindhoven, 2002.
- [15] TheEngineeringToolbox, Resources, Tools and Basic Information for Engineering and Design of Technical Applications, [www.engineeringtoolbox.com](http://www.engineeringtoolbox.com), visited 1-10-2012.
- [16] OmegaEngineering, Emissivity of Common Materials, <http://www.omega.com/literature/transactions/volume1/emissivityb.html>, 2012.
- [17] G. Tetzlaff, "Albedo of the Sahara," *Cologne Univ. Satellite Meas. of Radiation Budget*

*Parameters*, pp. 60-63, 1983.

- [18] I. Martínez, Heat Conduction, <http://webserver.dmt.upm.es/~isidoro/bk3/c11/Heat%20conduction.pdf>, 2012.
- [19] F. Kasten and A. Young, "Revised optical air mass tables and approximation formula," *Applied Optics*, no. 28, pp. 4735-4738, 1989.
- [20] M. Tukiainen, Sun path diagram Eindhoven, the Netherlands, [www.gaisma.com/en/location/eindhoven.html](http://www.gaisma.com/en/location/eindhoven.html), visited: 19-12-2012.
- [21] A. Meinel and M. Meinel, *Applied Solar Energy*, Addison Wesley Publishing Co, 1976.
- [22] 3M, "Factors Influencing the Optical Efficiency of Fresnel Lens Concentrators," Renewable Energy Division, St.Paul, 2009.
- [23] ShenZhen HaiWang Sensor Co. Ltd, Guangdong (China): <http://szhaiwang.en.alibaba.com/>, visited: 10-11-2012.
- [24] EG Solar Neuöttinger Str. 64c Altötting, Germany, [www.eg-solar.de](http://www.eg-solar.de), visited 01-10-2012.
- [25] P. Kinley, TWO-STAGE SOLAR CONCENTRATING SYSTEM, <http://www.rexresearch.com/kinley/kinley.htm>, visited: 12-11-2012.
- [26] SmartDrive, <http://www.smartdrive.co.uk/xyztable.html>, visited: 12-11-2012.
- [27] Robotic fiber optic laser welding machine JTWY-300F, Jiatai Laser: <http://www.jt-laser.net>, visited: 12-11-2012.
- [28] Philips, "Injection Molding for Solar Concentrators," in *CPV China 2012 & 4th International CPV Workshop*, [http://www.concentrating-pv.org/marburg2007/papers/19\\_Injection\\_Molding\\_for\\_solar\\_concentrators.pdf](http://www.concentrating-pv.org/marburg2007/papers/19_Injection_Molding_for_solar_concentrators.pdf), 12-10-2007.
- [29] R. Beardmore, Friction Coefficients, <http://www.roymech.co.uk>, visited: 13-11-2012.
- [30] R. Walker, Density of Materials, [www.simetric.co.uk](http://www.simetric.co.uk), 2011.
- [31] Unknown, "The Glass Transition," Polymer Science Learning Center, University of Southern Mississippi, 2005.

Cover image captured from: [http://www.cyberlawcentral.com/wp-content/uploads/2010/03/Libya\\_5230\\_Wan\\_Caza\\_Dunes\\_Luca\\_Galuzzi\\_2007.jpg](http://www.cyberlawcentral.com/wp-content/uploads/2010/03/Libya_5230_Wan_Caza_Dunes_Luca_Galuzzi_2007.jpg)

## 7 Appendix

Costs of materials for 3D sand printer

### FINAL COSTS Sand Printer

Category	Part	Specifications	Costs
Lens	Fresnel lens	1439*908 mm	€ 379.59
Electronics			
	MakerBot Gen 4 Electronics kit	Electronics including pulleys and timing belt	€ 317.69
	Arduino Uno for solar tracker		€ 24.20
	Stepper motor drivers for solar trackers	Drivers up to 2A phase current	€ 40.00
	Components for solar tracker (LDRs etc)		€ 10.60
Motors	Stepper motors	Nema 17; 4*gearbox 4:1, 1*16:1	€ 227.87
Wood	Wooden rotation disc	Water proof laminated, 2.5*1,25	€ 89.95
Steel		Construction steel for printer	€ 127.85
Bearings	Ball bearings for rail system	608 ABEC9 skate bearing (56pc)	€ 41.00
Import costs	Stepper motors	From China	€ 22.47
	Lens	From China	€ 79.38
	MakerBot Electronics kit	From Denmark	€ -
<b>TOTAL COSTS</b>			€ 1,360.60